

## Supplementary Information

### Understanding Trends in the Mercury Oxidation Activity of Single-Atom Catalysts

Weijie Yang<sup>a,b,c</sup>, Xuelu Chen<sup>a,b,c</sup>, Yajun Feng<sup>a,b,c</sup>, Fei Wang<sup>d</sup>, Zhengyang Gao<sup>a,b,c</sup>, Yanfeng Liu<sup>\*a,b,c</sup>, Xunlei Ding<sup>\*e,f</sup>, Hao Li<sup>\*g</sup>

<sup>a</sup> Department of Power Engineering, School of Energy, Power and Mechanical Engineering, North China Electric Power University, Baoding 071003, China

<sup>b</sup> Hebei Key Laboratory of Low Carbon and High Efficiency Power Generation Technology, North China Electric Power University, Baoding, 071003, Hebei, China

<sup>c</sup> Baoding Key Laboratory of Low Carbon and High Efficiency Power Generation Technology, North China Electric Power University, Baoding, 071003, Hebei, China

<sup>d</sup> Key Laboratory of Special Functional Materials for Ecological Environment and Information (Hebei University of Technology), Ministry of Education, Tianjin 300130, China

<sup>e</sup> School of Mathematics and Physics, North China Electric Power University, Beijing 102206, China.

<sup>f</sup> Institute of Clusters and Low Dimensional Nanomaterials, School of Mathematics and Physics, North China Electric Power University, Beijing, China.

<sup>g</sup> Advanced Institute for Materials Research (WPI-AIMR), Tohoku University, Sendai 980-8577, Japan.

#### \* Corresponding Authors:

Yanfeng Liu ([liuyanfeng@ncepu.edu.cn](mailto:liuyanfeng@ncepu.edu.cn))

Xunlei Ding ([dingxl@ncepu.edu.cn](mailto:dingxl@ncepu.edu.cn))

Hao Li ([li.hao.b8@tohoku.ac.jp](mailto:li.hao.b8@tohoku.ac.jp))

## Microkinetic modeling methods

In this study, we employed a microkinetic framework based on the Sabatier analysis<sup>1</sup> to find an upper bound of the overall reaction rate of Hg<sup>0</sup> oxidation. The Sabatier rate<sup>1</sup> is the reaction rate when each elementary reaction is assumed to be optimal, which can well reflect the catalytic reaction ability of the surface. This process is similar to the previously reported modeling for oxidation reactions<sup>2, 3</sup>. Based on the discussions in the main text, the reaction of Hg<sup>0</sup> oxidation can be divided into the following four elementary steps:



where R1 is assumed to be in equilibrium. The forward rate constants of the remaining steps are given by:

$$k_i = v_i \exp\left[\frac{-\Delta G_{ai}}{KT}\right] = v_i \exp\left[\frac{-(E_{ai} - T \Delta S_{ai})}{KT}\right], \quad (2)$$

where  $v_i$  is the prefactor,  $E_{ai}$  is the activation energy, and  $\Delta S_{ai}$  is the entropy difference between the transition state and the initial state,  $k$  is the Boltzmann constant, and  $T$  is the temperature.  $v_i$  is estimated by  $kT/h$ , where  $h$  is the Planck's constant.

Assuming R1 is in equilibrium, this gives:

$$\theta_{\text{O}_2} = \frac{1}{1 + K_1 p(\text{O}_2)}, \quad (5)$$

where  $K_i$  is the equilibrium constant of R1,  $p(\text{O}_2)$  is the partial pressure of O<sub>2</sub>.  $K_i$  was calculated by:

$$K_1 = \exp\left[\frac{-G_1}{kT}\right], \quad (6)$$

where  $G_1$  is the free energy of R1. The Sabatier rate ( $r_i^{S_{max}} = \theta_i k_i$ ) of the overall

reaction ( $r_S$ ) was estimated by the minimum reaction rate among R2-R4 as a function of O adsorption energy:

$$r_S = \text{Min}[r_2^{S_{max}}, r_3^{S_{max}}, r_4^{S_{max}}]. \quad (7)$$

Finally, the volcano activity plot is plotted as:

$$A = kT \ln[r_S h / kT]. \quad (8)$$

## References

1. T. Bligaard, J. K. Nørskov, S. Dahl, J. Matthiesen, C. H. Christensen and J. Sehested, The Brønsted–Evans–Polanyi relation and the volcano curve in heterogeneous catalysis, *Journal of Catalysis*, 2004, **224**, 206-217.
2. H. Li, A. Cao and J. K. Nørskov, Understanding Trends in Ethylene Epoxidation on Group IB Metals, *ACS Catalysis*, 2021, **11**, 12052-12057.
3. H. Falsig, B. Hvolbaek, I. S. Kristensen, T. Jiang, T. Bligaard, C. H. Christensen and J. K. Nørskov, Trends in the catalytic CO oxidation activity of nanoparticles, *Angewandte Chemie International Edition*, 2008, **47**, 4835-4839.

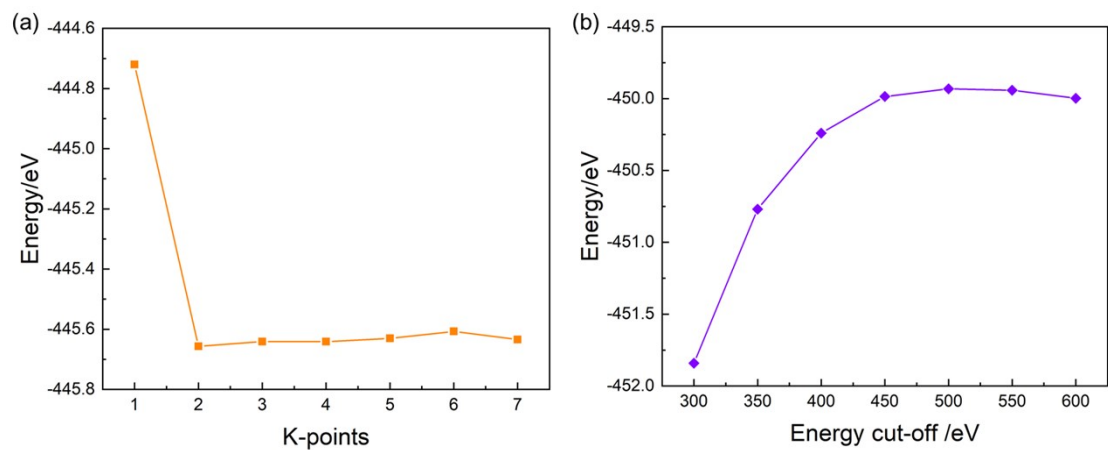


**Figure. S1.** Parameter test calculations on the settings of (a)  $k$ -points test (b) energy cutoff.

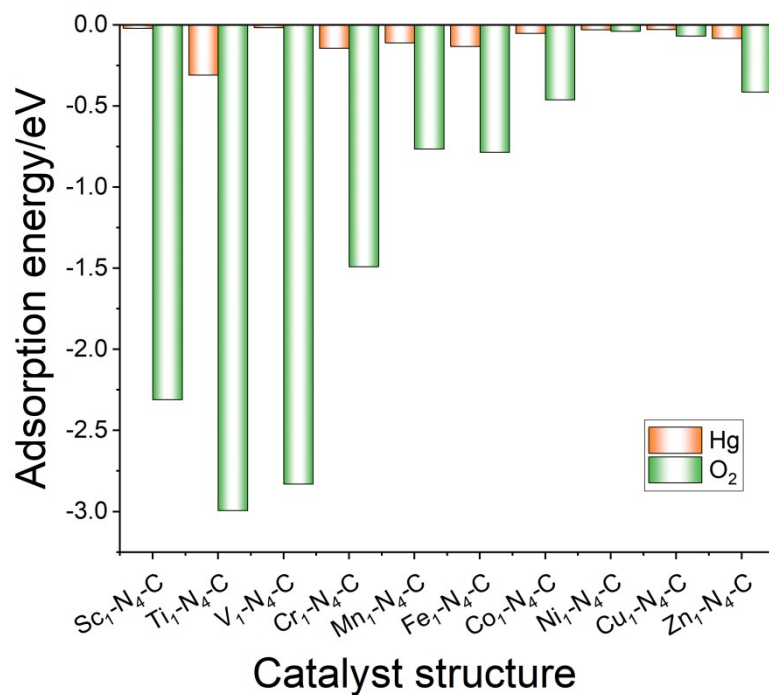


**Figure S2.** Adsorption energy of O<sub>2</sub> and Hg<sup>0</sup> on ten single-atom catalysts

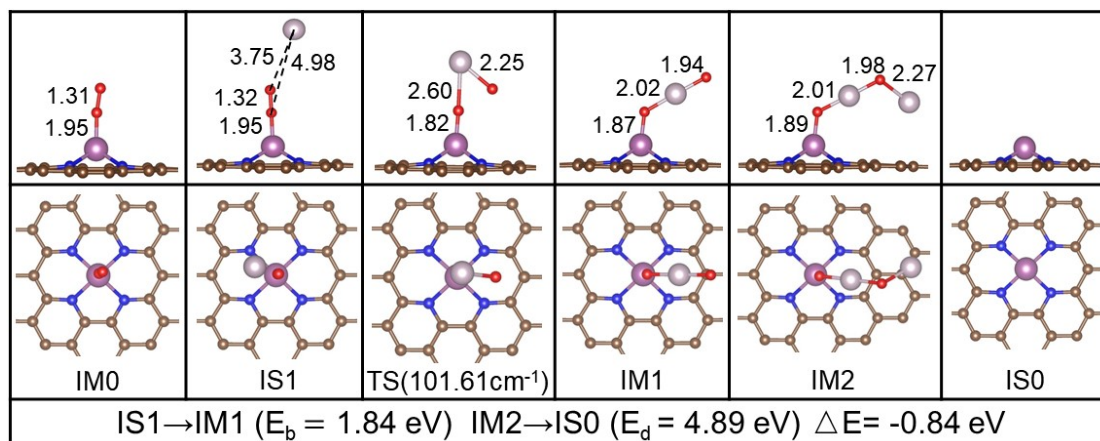


**Figure S3.** Reaction pathway of catalytic oxidation of  $\text{Hg}^0$  on  $\text{Sc}_1\text{-N}_4\text{-C}$ . C, N, and Sc are denoted by brown, blue, and pink, respectively.

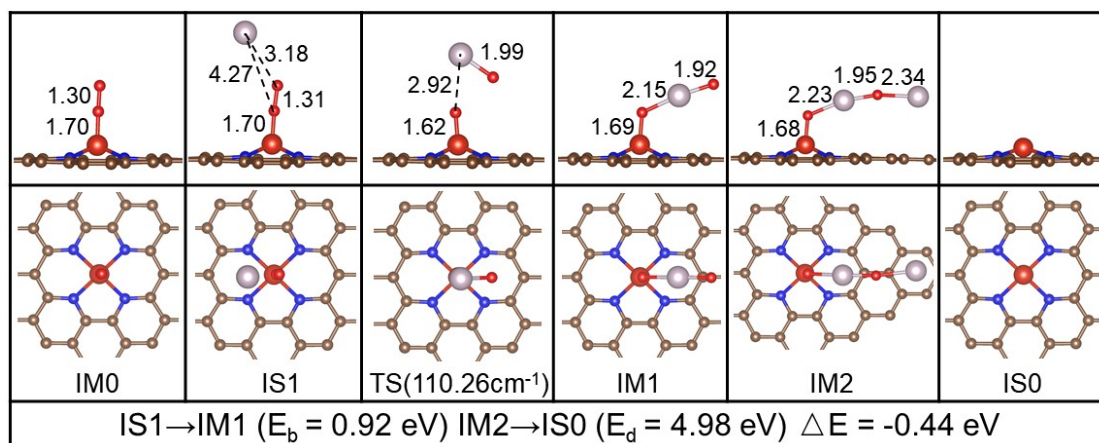


**Figure S4.** Reaction pathway of catalytic oxidation of Hg<sup>0</sup> on V<sub>1</sub>-N<sub>4</sub>-C. C, N, and V are denoted by brown, blue, and red, respectively.

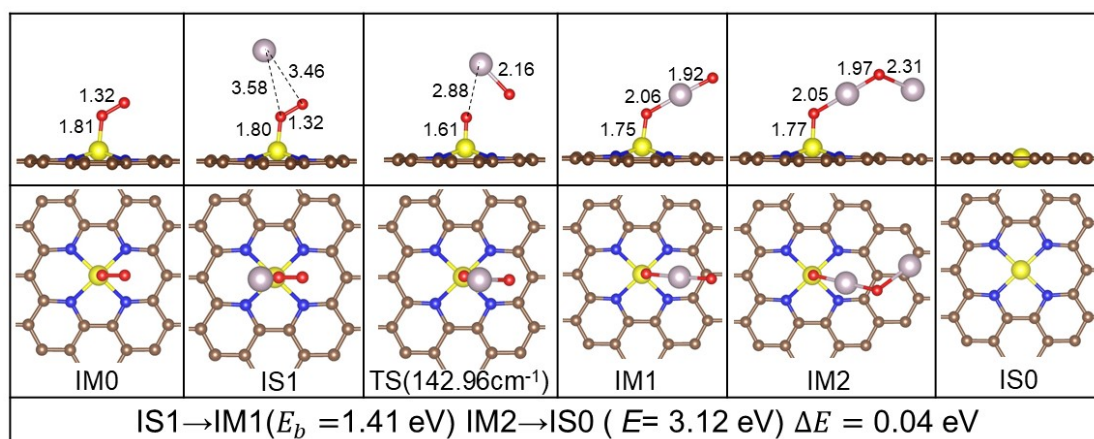


**Figure S5.** Reaction pathway of catalytic oxidation of  $Hg^0$  on  $Cr_1-N_4-C$ . C, N, and Cr are denoted by brown, blue, and yellow, respectively.

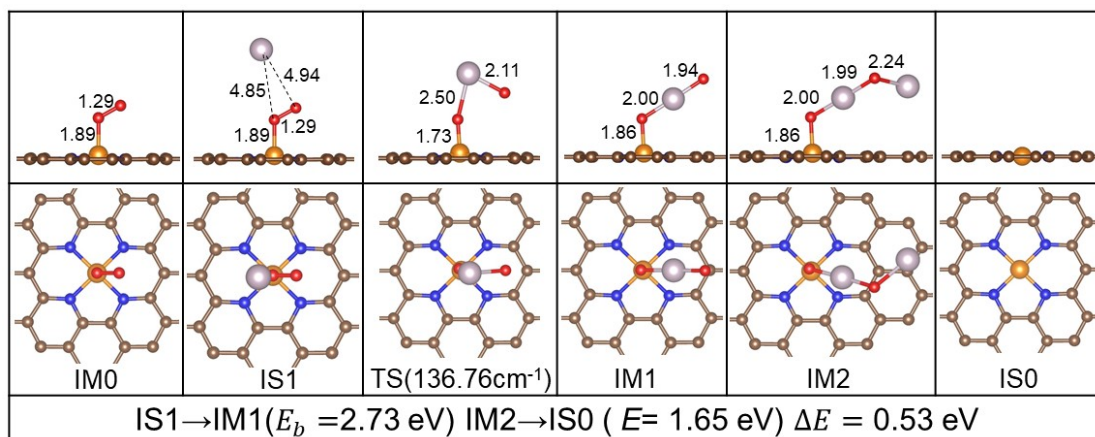


**Figure S6.** Reaction pathway of catalytic oxidation of  $\text{Hg}^0$  on  $\text{Co}_1\text{-N}_4\text{-C}$ . C, N, and Co are denoted by brown, blue, and orange, respectively.

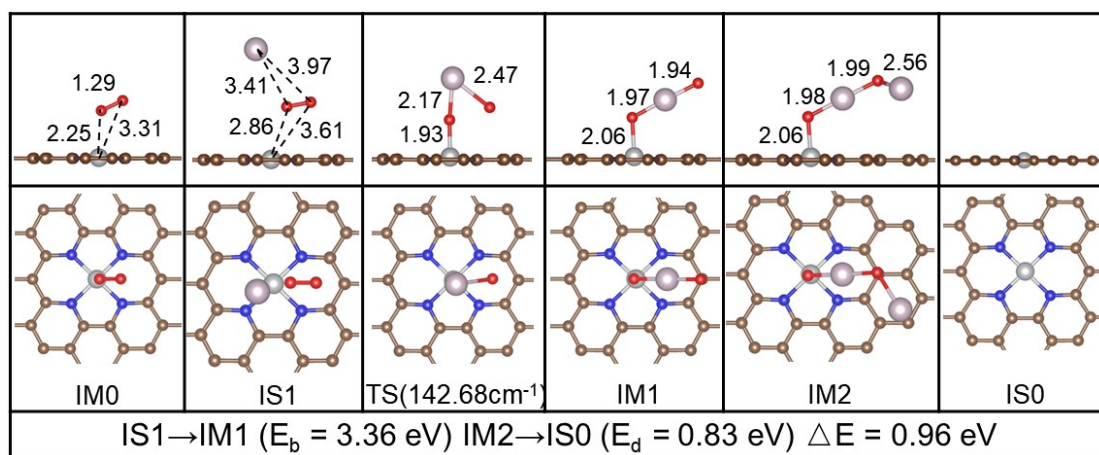


**Figure S7.** Reaction pathway of catalytic oxidation of  $Hg^0$  on  $Ni_1-N_4-C$ . C, N, and Ni are denoted by brown, blue, and light grey, respectively.

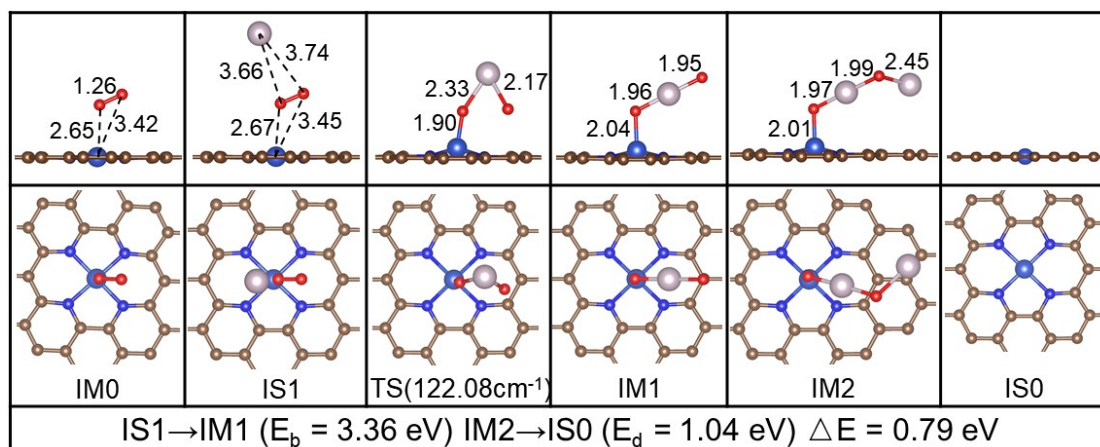


**Figure S8.** Reaction pathway of catalytic oxidation of  $Hg^0$  on  $Cu_1-N_4-C$ . C, N, and Cu are denoted by brown, blue, and light blue, respectively.

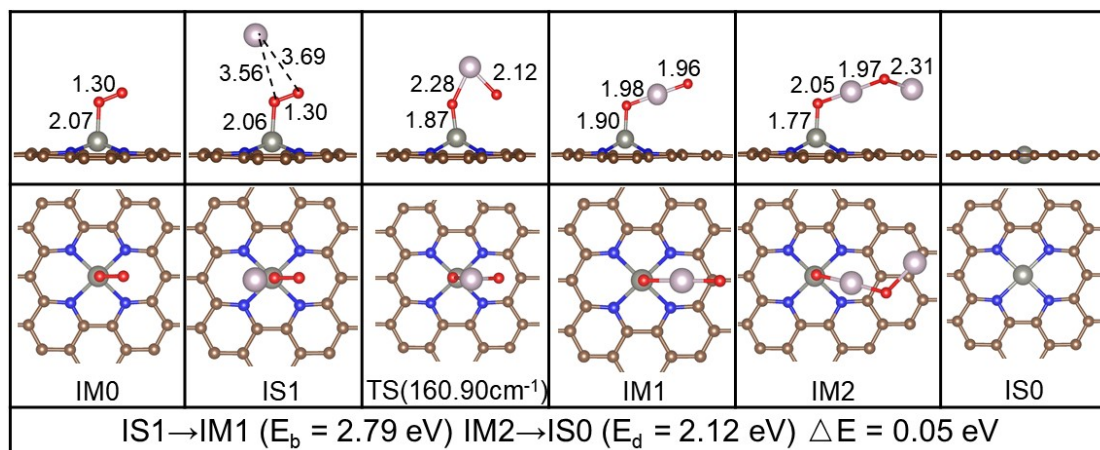


**Figure S9.** Reaction pathway of catalytic oxidation of Hg<sup>0</sup> on Zn<sub>1</sub>-N<sub>4</sub>-C. C, N, and Zn are denoted by brown, blue, and grey, respectively.

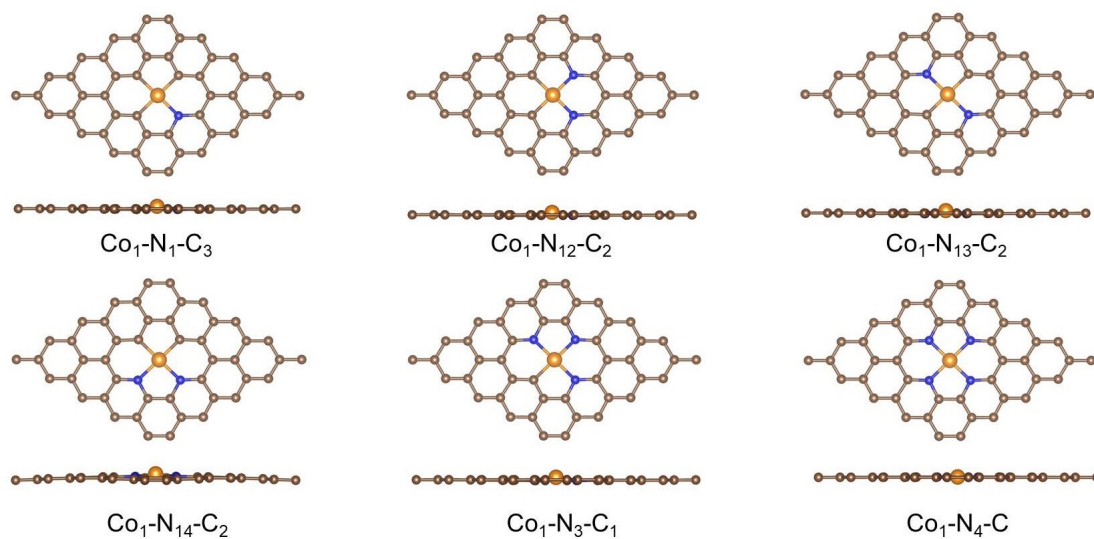


**Figure S10.** Optimized geometric structures of six Co-N-C catalysts. C, N, and Co are denoted by brown, blue, and orange, respectively.

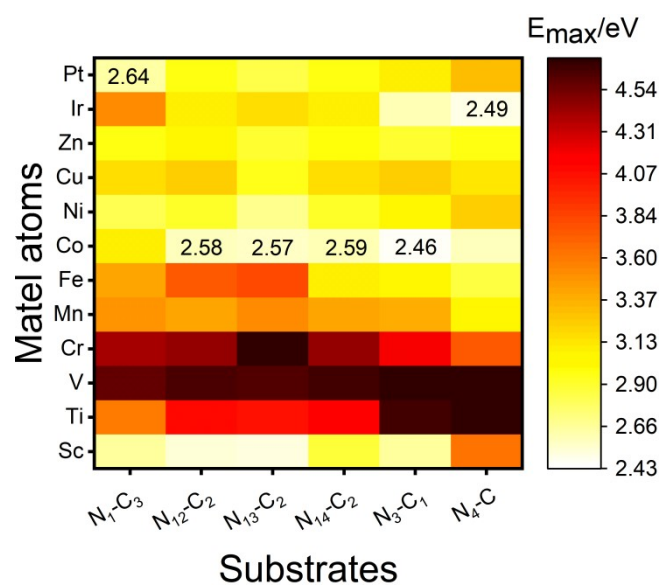


**Figure S11.** Predicted rate-determining step barriers for 72 SACs in the catalytic oxidation of  $Hg^0$ .

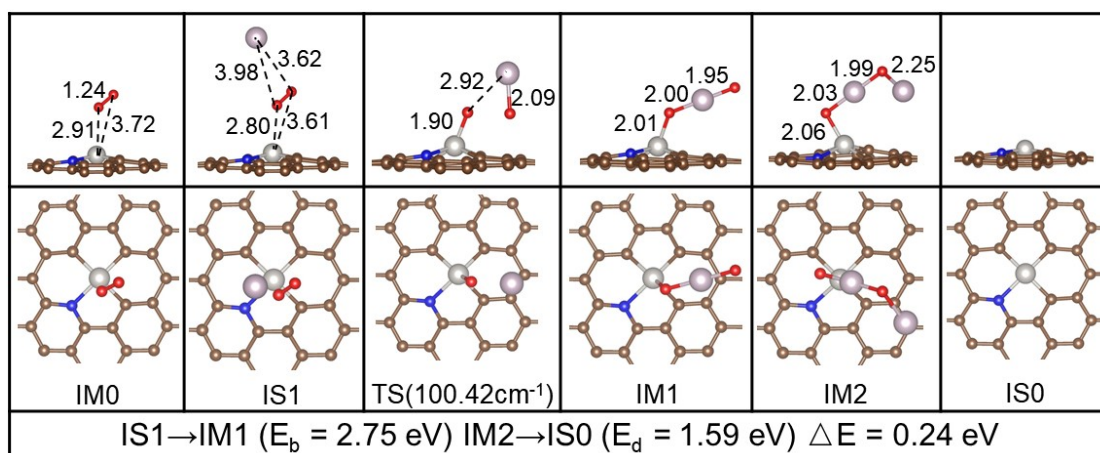


**Figure S12.** Reaction pathway of catalytic oxidation of  $\text{Hg}^0$  on  $\text{Pt}_1\text{-N}_1\text{-C}_3$ . C, N, and Pt are denoted by brown, blue, and silver white, respectively.

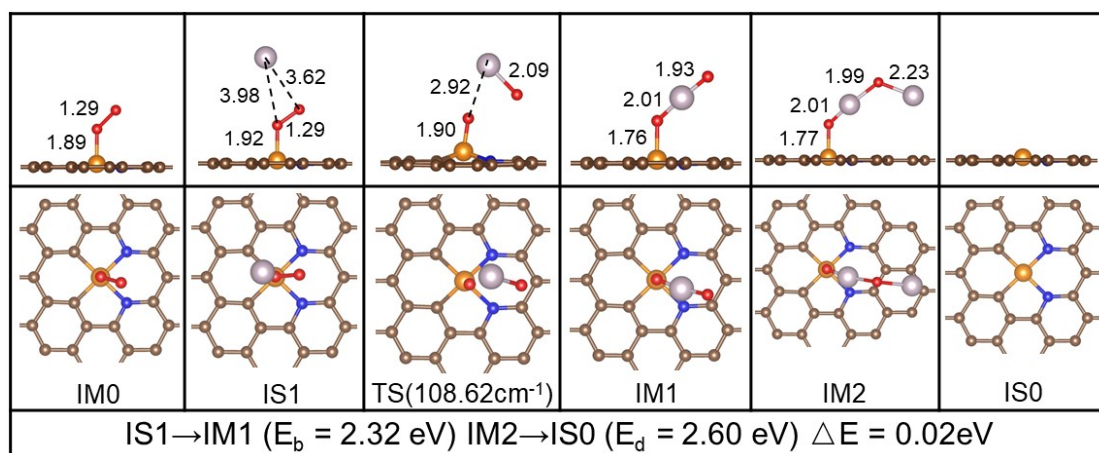


**Figure S13.** Reaction pathway of catalytic oxidation of Hg<sup>0</sup> on Co<sub>1</sub>-N<sub>12</sub>-C<sub>2</sub>. C, N, and Co are denoted by brown, blue, and orange, respectively.

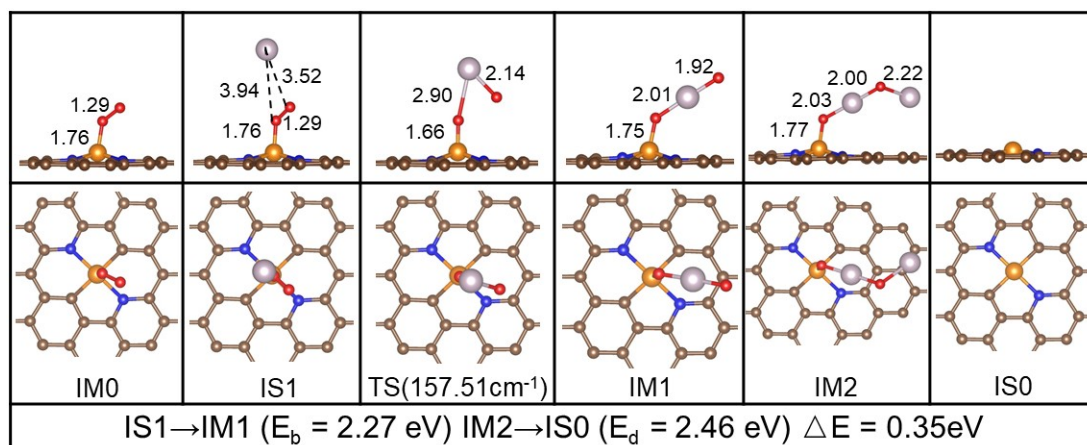


**Figure S14.** Reaction pathway of catalytic oxidation of Hg<sup>0</sup> on Co<sub>1</sub>-N<sub>13</sub>-C<sub>2</sub>. C, N, and Co are denoted by brown, blue, and orange, respectively.

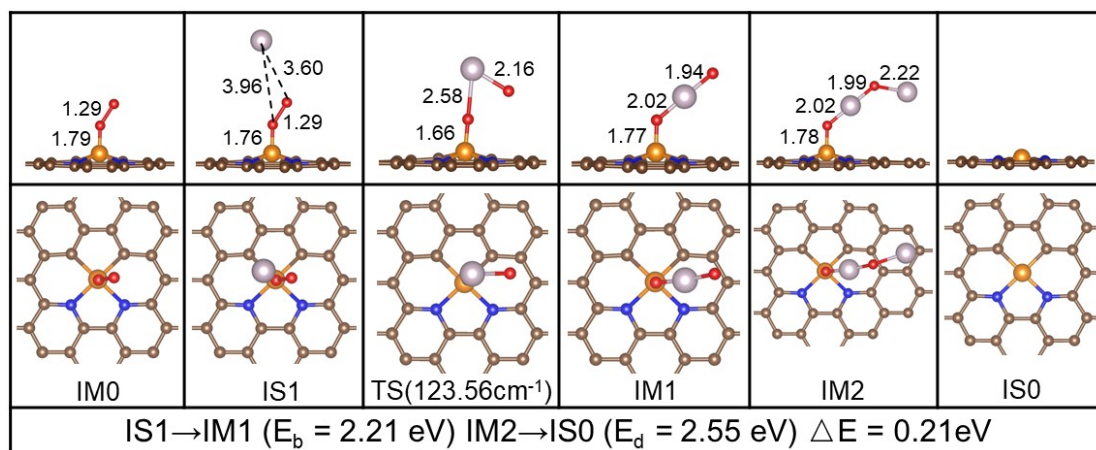


**Figure S15.** Reaction pathway of catalytic oxidation of Hg<sup>0</sup> on Co<sub>1</sub>-N<sub>14</sub>-C<sub>2</sub>. C, N, and Co are denoted by brown, blue, and orange, respectively.

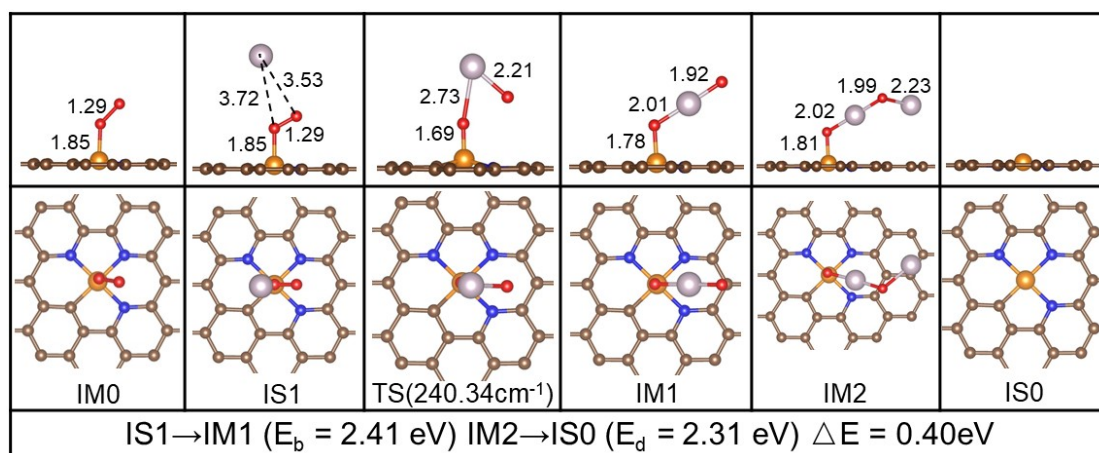


**Figure S16.** Reaction pathway of catalytic oxidation of  $\text{Hg}^0$  on  $\text{Co}_1\text{-N}_3\text{-C}_1$ . C, N, and Co are denoted by brown, blue, and orange, respectively.

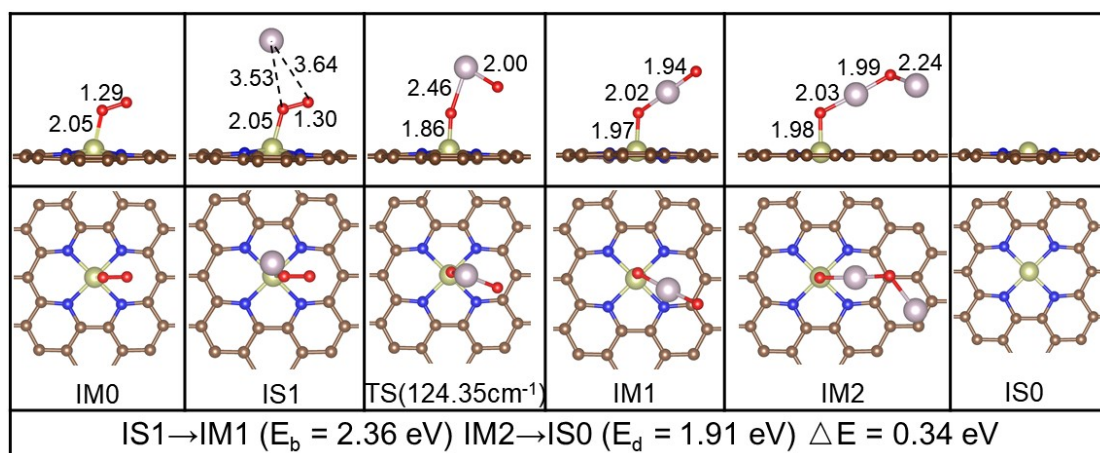


**Figure S17.** Reaction pathway of catalytic oxidation of Hg<sup>0</sup> on Ir<sub>1</sub>-N<sub>4</sub>-C. C, N, and Ir are denoted by brown, blue, and light yellow, respectively.